JOURNAL OF CATALYSIS 143, 481–491 (1993)

Oxygen Adsorption on Supported Silver Catalysts Investigated by Microgravimetric and Transient Techniques

DIMITRIS I. KONDARIDES AND XENOPHON E. VERYKIOS

Institute of Chemical Engineering and High Temperature Chemical Processes, and Department of Chemical Engineering, University of Patras, GR 26110 Patras, Greece

Received December 15, 1992; revised March 24, 1993

Oxygen adsorption on α-Al_2O_3-supported Ag catalysts was investigated in the temperature range 40 to 400°C. The adsorption kinetics, studied with a vacuum ultramicrobalance and analyzed with the Elovich equation, indicate that three kinetically distinguishable processes take place, with activation energies of ~1, 10.5, and 24 kcal/mol. Temperature-programmed desorption (TPD) experiments confirm the existence of three adsorbed oxygen species. A weakly adsorbed species, which is found to desorb below 150°C, is related to the 10.5 kcal/mol adsorption process and is assigned to molecularly adsorbed oxygen. The adsorption peak at 285°C is related to the almost nonactivated process and is ascribed to atomic oxygen, which is probably multicoordinated on the surface. At high adsorption temperatures (300 and 400°C) a third peak, desorbing above 400°C, is observed in the TPD profiles and is related to the highly activated process of 24 kcal/mol which is revealed by the gravimetric experiments. This species is suggested to be subsurface oxygen based on the results of TPD experiment conducted after isotope exchange of preadsorbed $^{16}O_2$ and $^{18}O_2$. Temperature-programmed reaction (TPR) experiments showed that all three species are active toward ethylene combustion.

INTRODUCTION

Silver is unique in its ability to selectively catalyze ethylene epoxidation, a process of significant industrial interest. The interaction of oxygen with silver surfaces under reaction conditions is one of the most controversial mechanistic aspects of the chemistry of this catalytic system (*1–3*). The adsorption of oxygen on Ag has been investigated employing a large variety of experimental techniques on single crystals (*4–11*), on silver films and foils (*12–16*), and on crystallites dispersed on metal oxide carriers (*17–22*). The effects of modifications of catalytically active surfaces by alloying or by surface promoters on the mode of oxygen adsorption have also been investigated (*21–25*).

It has been established, with many experimental techniques, that at cryogenic temperatures oxygen adsorbs on Ag surfaces nondissociatively (*5, 8, 13, 26, 27*). At elevated temperatures, two kinds of adsorbed atomic oxygen species have been identified, either mono- and multicoordinated (*21*) or species in a surface and subsurface state (*5, 7, 8, 26*). The latter is thought to play an indirect role in ethylene epoxidation/combusion chemistry, probably by reducing the bond energy between silver and adsorbed oxygen and converting the repulsive interaction between adsorbed oxygen and gas-phase ethylene into an attractive one (*28*).

There is strong evidence that under reaction conditions a diatomic oxygen species also exists in the adsorbed mode on the catalyst surface. Such a species has been proposed by Kilty *et al.* (*29*) and by Clarkson and Cyrillo (*30*). Grant and Lambert (*4*), using XPS and UPS, observed a molecular oxygen species on Ag (111), which was found to desorb at 380 K. Other investigators (*15, 18, 23*) also identified adsorbed diatomic oxygen species at temperatures as high as 200°C. Recently, high-quality Ra-

0021-9517/93 $5.00

man spectra were obtained in this laboratory after exposing Ag/ZrO_2, Ag/quartz and Ag/α-Al_2O_3 catalysts to oxygen (*32, 33*). A very intense peak located at 815 cm^{-1} was found to persist at temperatures as high as 620 K, exhibiting an isotope shift upon exposure to $^{18}O_2$ and was assigned to molecular oxygen (*32, 33*).

The specific role of each of these oxygen species adsorbed on silver surfaces in the mechanism of ethylene epoxidation and combustion has been a matter of controversy. Certain investigators believe that molecularly adsorbed oxygen participates in ethylene oxide formation, while others have proposed that molecular oxygen, although present, plays no direct role is either epoxidation or combustion routes and only the atomically adsorbed species is catalytically active.

In the present investigation the adsorption of oxygen on polycrystalline surfaces of Ag crystallites dispersed on an α-Al_2O_3 carrier is investigated employing microgravimetric, transient, isotopic labeling, and SERS (surface-enhanced Raman spectroscopy) techniques. The influence of geometric alterations of the catalytic surface by incorporation of Au atoms in the Ag surface matrix on the mode of oxygen adsorption is also investigated and related to mechanistic aspects of ethylene epoxidation and combustion. In the present paper, the adsorption of oxygen on Ag/α-Al_2O_3, as investigated with microgravimetric and desorption techniques, is discussed.

EXPERIMENTAL

The catalyst employed in the present investigation was prepared by impregnation of low surface area α-Al_2O_3, (Alfa Products) of a particle size of 40 μm and surface area of approximately 1 m^2/g with $AgNO_3$ (Merck, HCl free). A known amount of $AgNO_3$ was dissolved in water and the carrier was added to the solution under continuous stirring. The slurry was heated slowly to 70°C and maintained at that temperature until nearly all the water evaporated. The solid was then dried in an oven overnight at 110°C and the metal salt was reduced under hydrogen flow at 350°C for 8 h. The silver loading of the catalyst was 15 wt%.

The dynamic adsorption of oxygen on Ag/α-Al_2O_3 catalyst was studied with a vacuum microbalance (Cahn C-2000). The microbalance chamber was evacuated with a turbomolecular pump to an ultimate pressure of 10^{-6} Torr. The pressure in the chamber was measured and monitored with a high-accuracy pressure measurement and control system (MKS, 170 M). The catalyst, ground and sieved in the particle size range between 63 and 125 μm, was placed in a sample pan where it can be heated with a furnace connected to a temperature controller. Temperature is monitored with two K-type thermocouples, one placed just above the sample in the hangdown tube of the microbalance and the other in contact with the outer surface of the tube to control the furnace temperature. The microbalance is connected to a gas flow system which permits controlled introduction of O_2, H_2, or N_2 in the balance chamber. Weight changes are measured with the Cahn C-2000 microbalance weighing unit and are recorded with a personal computer which is connected to the balance via an interface module. Prior to each measurement the microbalance is properly calibrated with standard weights, supplied by the manufacturer.

The procedure involves placing approximately 330 mg of the catalyst powder in the sample pan, and heating the sample to 320°C under dynamic vacuum. A number of oxidation/reduction cycles were found to be necessary in order to obtain reproducible results. The sample was successively outgassed for 2 h, exposed to O_2 at 100 Torr for 5 h, outgassed for 2 h, and exposed to H_2 at 200 Torr for 5 h. This cycle was repeated approximately 10 times until the sample weight stabilized and reproducible adsorption curves were obtained. After these cycles the sample was heated at 320°C for 3 h, under dynamic vacuum, and then cooled to the adsorption temperature. A known pres-

sure of oxygen was introduced into the chamber and the sample weight was continuously recorded for 15 h. Oxygen adsorption experiments were conducted at temperatures between 40 and 320°C and at oxygen pressures between 15 and 200 Torr. Blank experiments with N_2, instead of O_2, were conducted under all experimental conditions in order to eliminate the effects of buoyancy and of the "initial shock" of the system upon introducing a gas into the evacuated chamber. The weight change which was observed upon N_2 introduction into the adsorption chamber during the initial 5 min was subtracted from that observed upon introduction of O_2.

The temperature-programmed desorption (TPD) and temperature-programmed reaction (TPR) experiments were carried out using an apparatus which has been described elsewhere (*34*). The catalyst sample, in powder form, was placed in a quartz microreactor where it was exposed to the same oxidation/reduction cycles as for the microgravimetric experiments. Ultrahigh purity He, further purified by passing it through oxygen and moisture traps was used as carrier gas, with a flow of 40 cm^3/min, during the TPD experiments. A 3.5% C_2H_4 in He mixture was used during the TPR experiments. Oxygen and/or CO_2, C_2H_4, and C_2H_4O at the effluent of the microreactor were detected using a Sensorlab 2000 D VG quadrupole mass spectrometer interfaced to a personal computer. After pretreatment of the catalyst, the sample was cooled to the desired temperature and exposed to O_2 flow for 30 min. It was then cooled to room temperature under O_2 flow. Oxygen adsorption was conducted at various temperatures between 25 and 400°C. Gas-phase oxygen was purged from the tubing, bypassing the reactor, until the oxygen baseline was obtained in the mass spectrometer. The microreactor was then purged with He flow for 3 min. The sample was subsequently heated, with a heating rate of 20°C/min under 40 cm^3/min He flow for the TPD experiments or under 40 cm^3/min of 3.5% C_2H_4/He flow for the TPR experiments. Isotope-exchange experiments using $^{18}O_2$ were conducted as follows. After adsorbing $^{16}O_2$ for 30 min at the desired temperature, as described above, the flow was switched to N_2 for 5 min to remove gas-phase oxygen, and then to 0.97% $^{18}O_2/N_2$. The transient behavior of $^{16}O_2$, $^{18}O_2$, and $^{16}O^{18}O$ was monitored for 5 min. The sample was then quickly cooled to 30°C under $^{18}O_2/N_2$ flow and a TPD experiment was conducted. The mass spectrometer signal of all species of interest was properly calibrated using dilute gas streams of known concentration.

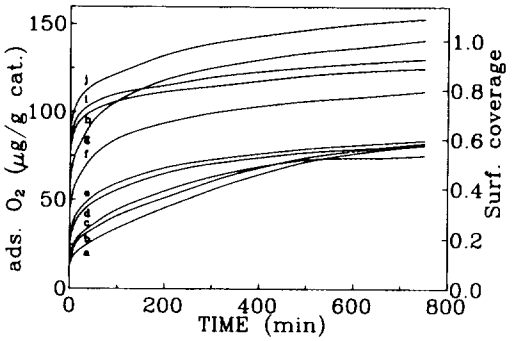

FIG. 1. The adsorption of oxygen on reduced Ag/α-Al_2O_3 at various temperatures: (a) 40, (b) 70, (c) 100, (d) 130, (e) 165, (f) 180, (g) 200, (h) 240, (i) 280, and (j) 320°C; oxygen pressure: 50 Torr.

RESULTS AND DISCUSSION

(*a*) *Kinetics of Oxygen Adsorption on Ag/α-Al_2O_3 Catalyst*

The rate of oxygen adsorption on α-Al_2O_3-supported Ag particles was determined in the temperature range 40 to 320°C, at constant oxygen pressures between 15 and 200 Torr, following the procedure described earlier. The temperature dependence of the oxygen adsorption rate at a pressure of 50 Torr is illustrated in Fig. 1 in the form of mass uptake versus time for different temperatures. A very rapid initial oxygen uptake is observed at all temperatures, upon exposure of the catalyst surface to oxygen. Adsorption continues, but at a significantly reduced rate, for several hours. The saturation

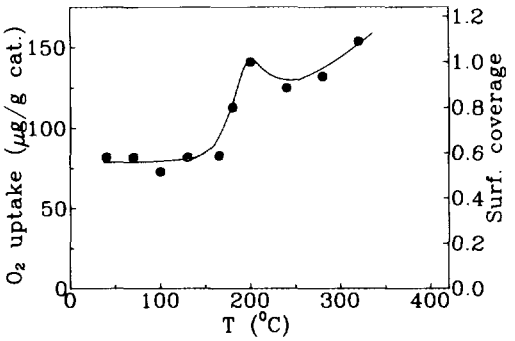

FIG. 2. The temperature dependence of the oxygen saturation uptake. P_{O_2} = 50 Torr.

uptake plotted against the adsorption temperature is shown in Fig. 2. It is interesting to observe that at temperatures below 165°C, the adsorption curves reach a saturation value of approximately 80 μg of adsorbed oxygen per gram of catalyst. A significant increase in the saturation oxygen uptake is observed at adsorption temperatures between 165 and 200°C. This might indicate the initiation of a new adsorption process, which is activated and thus becomes dominant at temperatures higher than 165°C while, at lower temperatures, its contribution to oxygen uptake is negligible. At temperatures higher than 200°C the saturation uptake is decreased, indicating that desorption of an adsorbed oxygen species becomes significant and saturation uptake is governed by equilibrium considerations. At even higher temperatures, the O_2 uptake increases further, indicating the onset of a new process, not necessarily related to adsorption. This new uptake process is probably related to dissolution of oxygen in the bulk of the metal and it becomes measurable at temperatures above 240°C. Oxygen uptake at temperatures higher than 240°C was found to increase monotonically with temperature, indicating that this uptake is not governed by adsorption equilibrium constraints. The maximum oxygen uptake of ~140 μg per gram of catalyst observed at 200°C was considered to correspond to monolayer coverage.

Attempts were made to analyze the adsorption curves of Fig. 3 following various kinetic expressions including Langmuir equations of nth order. These kinetic expressions failed to describe, in any accurate manner, the experimental curves of Fig. 1. However, the rate of oxygen adsorption on α-Al_2O_3-supported silver catalysts can be described using the Elovich equation (*35*), which is of the form

$$r = \frac{d\Theta}{dt} = \beta P e^{-\gamma\Theta}, \qquad (1)$$

where r is the rate of adsorption, Θ is the oxygen surface coverage at any time t, and P is the oxygen pressure in the chamber, while β and γ are temperature-dependent parameters described by

$$\beta = k_a f(\Theta) \exp(-E_0/RT) \qquad (2)$$

$$\gamma = \gamma_0/RT, \qquad (3)$$

in which k_a is the specific rate constant of adsorption, E_0 is the activation energy of adsorption at zero surface coverage, and γ_0 is a constant.

The Elovich equation has been derived under the following assumptions (*36*): (a) the adsorbent has a homogeneous surface; (b) the activation energy of adsorption increases linearly with surface coverage, Θ; (c) the function $f(\Theta)$ varies far more slowly than exponentially so that in the course of adsorption it may be considered to be con-

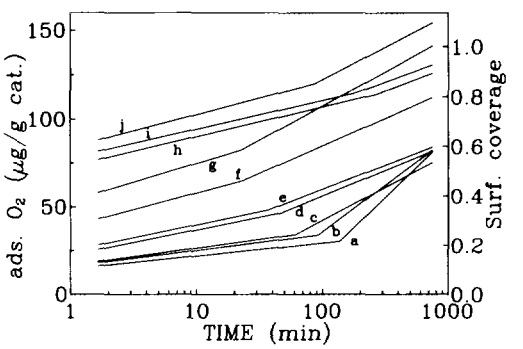

FIG. 3. Adsorption curves of Fig. 1 plotted in the coordinates of the integrated Elovich equation.

stant; (d) pressure is constant in the course of adsorption; and (e) the rate of adsorption is far greater than the rate of desorption. Based on these assumptions, the Elovich equation can be integrated to the form

$$\Theta = \frac{1}{\gamma}\ln(t + t_0) - \frac{1}{\gamma}\ln t_0, \qquad (4)$$

where t_0 is a parameter defined by

$$t_0 = (\beta\gamma P)^{-1}. \qquad (5)$$

Adsorption curves plotted in the coordinates of the integrated Elovich equation are shown in Fig. 3. It is apparent that the linearity of Eq. (4) is satisfied. However, each curve on this figure consists of two intersecting straight lines, indicating the existence of at least two distinctive adsorption processes. At adsorption temperatures below 200°C, the point of intersection of the two linear segments occurs at low surface coverages, between 0.2 and 0.4, and high time values and it moves toward higher surface coverages and lower time values with increasing temperature of adsorption. A shift of the break-point is observed at adsorption temperatures between 200 and 240°C, toward significantly higher surface coverages and time values. This break-point is probably not related to that observed at temperatures below 200°C. It is at the temperature range 200 to 240°C where the uptake process which does not resemble adsorption, as discussed earlier, is initiated. Thus the break-point of the high-temperature lines probably differentiates this uptake process from that of the adsorption process. The break which is observed in the low-temperature lines might also be present in the high-temperature cases but occurring at very low time values, thus being undetectable with the gravimetric system used in these experiments.

The values of the parameters β and γ can be estimated from the slopes and intersects of the linear segments of Fig. 3. The activation energy of oxygen adsorption at zero surface coverage, E_0, can then be estimated according to Eq. (2). The Arrhenius-type

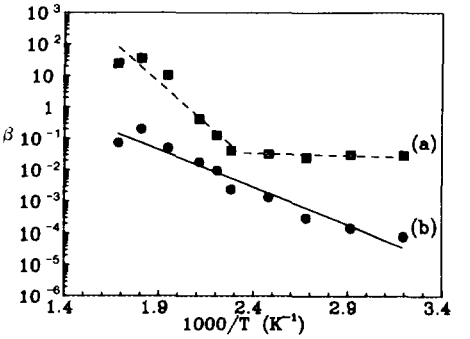

FIG. 4. Arrhenius plot of the Elovich parameter β calculated from the intersections of the first (low time values) and second (high time values) line segments of Fig. 3.

plot of the adsorption curves of Fig. 3 is shown in Fig. 4. It is apparent that the data of the first (low time values) linear segment reveal two distinct and widely different adsorption processes. One with a very low activation energy, approximately 1 kcal/mol, which essentially describes a nonactivated adsorption process taking place at low temperatures (below 180°C) and low surface coverages. A second one with a high activation energy, approximately 24 kcal/mol, which describes a process taking place at high temperatures is also apparent. The data of the second (high time values) linear segment reveal a single activation energy of adsorption which is approximately 10.5 kcal/mol and describes an adsorption process which takes place at high surface coverages over the entire temperature range.

The pressure dependence of the adsorption rate was investigated at 200°C, in the pressure range 15 to 200 Torr. Oxygen uptakes versus time at pressures of 15, 50, 100, and 200 Torr are shown in Fig. 5. As expected, O_2 uptake increases with increasing pressure. The same data, plotted in the coordinates of the integrated Elovich equation, are shown in the inset of Fig. 5. Again, two intersecting straight lines are observed. The point of intersection moves to lower time values as the oxygen pressure increases but occurs at approximately the

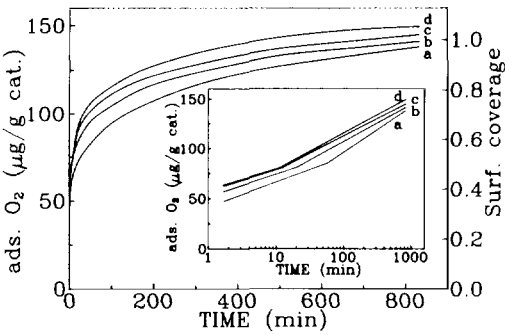

FIG. 5. The pressure dependence of the oxygen adsorption rate at 200°C under oxygen pressure of (a) 15, (b) 50, (c) 100, and (d) 200 Torr. Inset: The same data plotted in the coordinates of the integrated Elovich equation.

same coverage, indicating that the transition from one mode of oxygen adsorption to another is coverage-dependent and not pressure-dependent. As shown earlier, the surface coverage at the point of transition is temperature dependent, increasing with increasing temperature.

The results obtained from the microgravimetric experiments of O_2 adsorption on Ag surfaces reveal three distinct adsorption processes. The first one is dominant at low temperatures (<160°C) and low surface coverages (<0.4). At zero surface coverage this process is essentially nonactivated, since its activation energy, E_0, is only 1 kcal/mol. However, the activation energy is strongly dependent on surface coverage since the value of γ_0 is found to be 21.6 ± 3.4. With respect to surface coverage, the apparent activation energy of this process is: $E = 1 + 21.6\,\Theta$, kcal/mol $0 < \Theta < 0.4$. This high value of γ_0 cannot be explained considering alterations in surface electronic properties, such as in the work function of surface metal atoms, caused by the adsorption of oxygen species. It probably implies that the already adsorbed oxygen species offer a stereochemical resistance to the adsorption of new oxygen species which is manifested as increased activation energy at higher surface coverages. Mechanistically this process can be explained as dissociative oxygen adsorption with oxygen adatoms occupying multiatom sites, such as tetrahedral sites, as has been proposed by other investigators (*21, 29, 31*). The high value of the activation energy at nonzero surface coverage is then describing the activation energy of formation of suitable adsorption sites as by surface rearrangement (diffusion) of the already adsorbed oxygen atoms.

A second mode of O_2 adsorption occurs at all temperatures and it is dominant at relatively high values of Θ. This is an activated process with an activation energy of 10.5 kcal/mol at zero surface coverage. The coverage-dependence of the activation energy of this process is significantly weaker, since the value of γ_0 obtained is 9.3. It is interesting to note that this mode of oxygen adsorption occurs over the entire temperature range investigated, 40–320°C. Based on these observations, this adsorbed oxygen species is correlated to the dioxygen species observed previously in this laboratory using surface enhanced Raman spectroscopy (SERS) (*32, 33*). A Raman band at 815 cm^{-1} was observed upon oxygen adsorption on supported Ag crystallites, which persisted at temperatures as high as 350°C. The intensity of this peak was observed to increase with time of exposure of the surface to oxygen. The fact that this band is indeed due to a dioxygen species was confirmed by isotopic labeling experiments. A shift in wavelength by about 20 cm^{-1} was observed upon exposure of the sample to $^{18}O_2$. Thus, it is proposed that the adsorbed species, which originates in the adsorption process of 10.5 kcal/mol activation energy at zero surface coverage, is a molecular one which lies perpendicular to the silver surface, in agreement with results obtained by other investigators (*29*).

The third oxygen adsorption process occurs at high temperatures with an activation energy of 24 kcal/mol at zero surface coverage. The results obtained by the microgravimetric adsorption experiments do not give any indications as to the nature of this ad-

sorbed species. It should be stated that the activation energy observed is probably too high to be attributed solely to an adsorption step. Since this process occurs at high temperatures, it can be related to oxygen dissolution into the bulk of the Ag particles, as discussed earlier.

(b) Temperature-Programmed Desorption and Reaction Studies

The adsorption/desorption characteristics of oxygen on α-Al_2O_3-supported Ag crystallites were also investigated employing TPD and TPR techniques. Oxygen adsorption was conducted by exposing the sample to O_2 flow at temperatures between 30 and 400°C, cooling rapidly to room temperature under O_2 flow, switching the flow to He, maintaining for 3 min, and then heating with a rate of 20°C/min under He flow. TPD profiles ("spectra") obtained following this procedure, after adsorption at 30, 100, 200, 300, and 400°C, are shown in Fig. 6. A weakly adsorbed O_2 species is observed to desorb at low temperatures. The fact that the O_2 detected in the temperature range 30 to 200°C does not originate from gas phase O_2 which has remained in the lines or the reactor was confirmed with blank experiments using unmetallized α-Al_2O_3. The weakly adsorbed oxygen appears at all adsorption temperatures, since the sample was cooled to room temperature under oxygen flow. At adsorption temperatures higher than 100°C, a second desorption peak is apparent with peak maximum between 270 and 330°C. A small shift of the peak maximum toward lower temperatures with increasing temperature of adsorption is also apparent. At adsorption temperatures of 300 and 400°C, a third desorption peak is apparent whose relative magnitude is significantly larger at 400°C. The temperature of initiation of the third peak is the same in both cases (~355°C) and the apparent shift in peak maximum is probably due to the significantly larger quantity of O_2 desorbing following adsorption at 400°C, as compared to the same quantity following adsorption at 300°C.

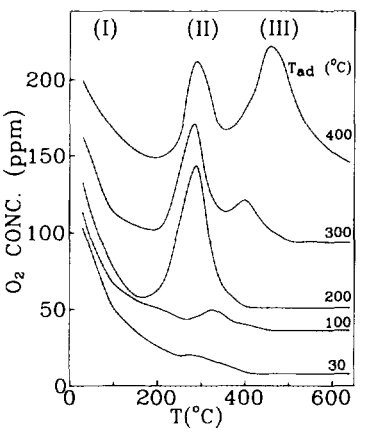

FIG. 6. TPD spectra obtained after oxygen adsorption at 30, 100, 200, 300, and 400°C for t = 30 min.

TABLE 1

Amount of Oxygen Desorbed after Adsorption at Temperatures between 30 and 400°C

Adsorption temperature (°C)	Total oxygen desorbed (μg/g)	Oxygen desorbed above 200°C (μg/g)
30	36.0	13.8
100	36.6	17.6
200	55.8	38.7
300	52.0	37.0
400	73.4	60.0

The quantities of O_2 detected to desorb after adsorption at various temperatures are reported in Table 1. The total quantity of O_2 desorbed follows exactly the same trend as that observed with the gravimetric adsorption method (Fig. 1): it increases up to an adsorption temperature of 200°C, then decreases at 300°C to increase again to a level higher than that of 200°C, when adsorption occurs at 400°C. The quantity of oxygen desorbed at temperatures below 200°C (weakly adsorbed) decreases monotonically with increasing adsorption temperature. This weakly adsorbed species might adsorb on vacant sites during cooling of the sample to room temperature under O_2 flow, prior to initiation of the TPD experiment.

The quantity of O_2 desorbing at temperatures above 200°C increases with increasing adsorption temperature up to 200°C, decreases slightly at T_{ad} of 300°C, probably for thermodynamic reasons, while at T_{ad} of 400°C it is significantly enhanced. This implies that at high adsorption temperatures a new O_2 uptake process is initiated which is not restricted by thermodynamic equilibrium adsorption constraints. An identical conclusion was also obtained from analysis of the microgravimetric adsorption curves.

Two distinct desorption peaks are observed at temperatures higher than 200°C, when adsorption takes place at temperatures of 300 and 400°C. Peak II decreases in magnitude with increasing temperature of adsorption between 200 and 400°C. This is probably due to equilibrium constraints. At a T_d of 300°C, a third peak appears (Peak III) at higher temperatures. At T_{ad} of 400°C the third peak has grown significantly and it is nearly twice the size of Peak II. The third desorption peak then arises from the uptake process which is not an adsorption process, as stated earlier. Peak III, which appears only at temperatures of adsorption higher than 300°C is probably due to dissolution of oxygen into the subsurface region, as has been suggested by other investigators (*5*, *8*).

The results of the TPD experiments are in good agreement with the results of the microgravimetric adsorption studies. In both cases, three distinct oxygen species were found to adsorb or desorb from Ag surfaces. Species I of the desorption spectra of Fig. 6 has many similarities with the species found to adsorb with an activation energy of 10.5 kcal/mol in the microgravimetric studies. This adsorbed oxygen species has been proposed to be a diatomic one. Peak II corresponds to desorption of the species adsorbing with an activation energy of 1 kcal/mol at zero surface coverage which has been attributed to dissociative adsorption with oxygen adatoms occupying multiatom sites on the surface. Finally, Peak III corresponds to the oxygen adsorption process observed to take place at high temperatures with an activation energy of 24 kcal/mol. Thus, this value of the activation energy of the process does not correspond to an adsorption but rather a diffusion step. This explains its rather high value.

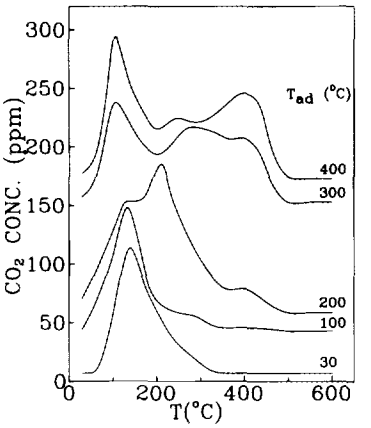

FIG. 7. Temperature-programmed reaction (TPR) spectra obtained after oxygen adsorption at 30, 100, 200, 300, and 400°C for 30 min and exposure to 3.5% C_2H_4/He.

The reactivity of oxygen adsorbed on Ag surfaces was investigated using ethylene as reactant under temperature-programmed reaction conditions. Adsorption was conducted at temperatures between 30 and 400°C, as described earlier. After cooling to 30°C, the sample was exposed to a flow of 3.5% C_2H_4 in He mixture and temperature programming was initiated. TPR spectra obtained are shown in Fig. 7. No measurable quantities of O_2 desorbing were detected, while CO_2 was the only reaction product detected. The curves corresponding to T_{ad} of 30 and 100°C clearly demonstrate that the weakly adsorbed oxygen species is active in C_2H_4 combustion. The low-temperature CO_2 peak exhibits a maximum which is shifted to lower temperatures (150 to 100°C) with increasing temperature of adsorption. This might imply that the reactivity of this adsorbed oxygen species towards ethylene combustion is affected by the presence of other adsorbed species on the catalyst sur-

face. The TPR spectrum which corresponds to oxygen adsorption at 200°C shows an intense CO_2 peak at approximately 210°C in addition to the low temperature peak (at ~120°C) as well as a small peak at approximately 420°C. Three TPR peaks of CO_2 are observed at O_2 adsorption temperatures of 300 and 400°C, which probably correspond to the three modes of adsorbed oxygen described earlier. The third (highest temperature) peak increases in intensity with increasing T_{ad}. This peak appears even at T_{ad} of 200°C as a shoulder to the main peak. In general, the TPR spectra of Fig. 7 resemble rather closely the TPD spectra of Fig. 6, indicating that all three oxygen species which exist on Ag catalysts are active toward C_2H_4 combustion. This conclusion is supported by the fact that no oxygen was detected to desorb during the TPR experiments. However, from these results it cannot be concluded whether all adsorbed oxygen species participate in C_2H_4 combustion directly from their adsorbed state or whether they are transformed into a different adsorbed state during the experiment, prior to their participation in C_2H_4 combustion. It is interesting to note that no ethylene oxide was detected in the gas phase under these experimental conditions. It should also be noted that the catalyst employed in the present study results in formation of significant quantities of ethylene oxide, exhibiting a selectivity of 50–70%, under steady-state reaction conditions. These observations imply that under TPR conditions ethylene oxide is either not formed or that it is rapidly oxidized further to CO_2 and water. Taking into consideration the fact that the contact time in the TPR and steady-state experiments was not significantly different, it can be concluded that the working state of the catalyst under TPR conditions is significantly different than that under steady-state reaction conditions.

(c) *Isotopic Labeling Experiments*

Isotope exchange experiments were also conducted at 200, 300, and 400°C. After $^{16}O_2$ adsorption at each temperature for 30 min, the flow over the catalyst was switched to N_2 for 5 min to remove gas-phase oxygen and then to 0.97% $^{18}O_2/N_2$. The transient behavior of $^{18}O_2$ and $^{16}O^{18}O$ obtained at 200, 300, and 400°C is shown is Fig. 8. These spectra indicate that significant isotope exchange takes place only at 400°C, much less at 300°C and that negligible exchange occurs at 200°C. This observation is reasonable since atomic oxygen is strongly held to the surface and desorbs close to 300°C in the absence of gas phase oxygen as shown in the TPD experiments (Fig. 6). It is expected that under the 0.97% $^{18}O_2/N_2$ flow the adsorption/desorption equilibrium will shift to higher temperatures and significant isotope exchange will take place only above 300°C. The isotope-exchange experiments were followed by TPD, after cooling the sample to room temperature under $^{18}O_2$ flow. The TPD spectra obtained following $^{16}O_2$ adsorption and isotopic exchange at 200, 300 and 400°C are shown in Fig. 9. Two desorption peaks of $^{16}O^{18}O$ and $^{18}O_2$ are apparent (the $^{16}O_2$ peaks are not shown) in the experiments conducted at 400 and 300°C, while a single oxygen peak appears at the adsorption temperature 200°C. No weakly adsorbed $^{16}O^{18}O$ molecular species is observed to desorb (expected at temperatures below 150°C). However, small quantities of $^{18}O_2$

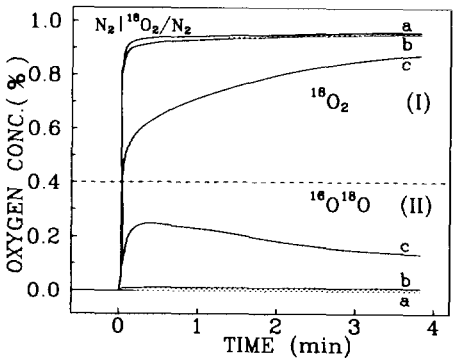

FIG. 8. The transient behaviour of $^{18}O_2$ and $^{16}O^{18}O$ under the sequence $^{16}O_2$ (30 min), N_2 (5 min) → 0.97% $^{18}O_2/N_2$ at temperatures of (a) 200, (b) 300, and (c) 400°C.

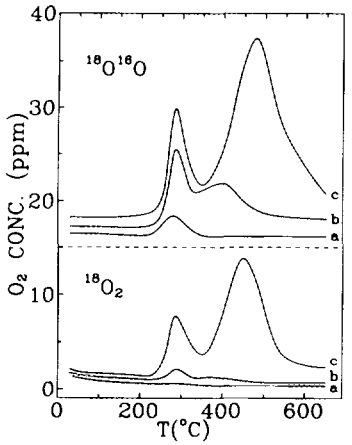

FIG. 9. TPD spectra obtained after $^{16}O_2$ adsorption at (a) 200, (b) 300, and (c) 400°C for 30 min followed by exposure to 0.97% $^{18}O_2/N_2$ for 5 min at the same temperatures.

are detected to desorb in the low-temperature region. This observation supports the idea that molecular oxygen adsorbs during cooling down to room temperature in sites not occupied by the other species. In these experiments the sample was cooled quickly under 0.97% $^{18}O_2/N_2$ flow, in contrast to the experiments of Fig. 6 in which the catalyst was cooled at a lower rate under pure O_2 flow. This 100-fold difference in oxygen pressure along with the different time of exposure during the cooling down period may be responsible for the decreased population of this species. In fact, Grant and Lambert (*4*) have found that the molecularly adsorbed oxygen coverage is indeed pressure dependent. The high-temperature peak is clearly resolved only when the exchange takes place at 400°C. The low-temperature peak of $^{16}O^{18}O$ and $^{18}O_2$ exhibits a maximum at exactly the same temperature (~285°C). However, the high-temperature peak of $^{16}O^{18}O$ is shifted by approximately 25°C higher than the corresponding peak of $^{18}O_2$. This observation implies that the ^{16}O adatom delays the process of desorption of the $^{16}O^{18}O$ species in which it participates. This can be explained assuming that the oxygen species desorbing at approximately 450°C is a subsurface one. The ^{16}O species is deeper into the bulk of the solid, while the ^{18}O species is closer to the surface. Thus $^{18}O_2$ desorbs more easily (at lower temperatures) than the $^{16}O^{18}O$ species which is delayed by ^{16}O diffusion from the bulk towards the surface. This is an additional indication that the high-temperature oxygen peak observed in the TPD experiments corresponds to oxygen dissolved in the Ag crystallites, or to subsurface oxygen.

CONCLUSIONS

The interaction of oxygen with surfaces of supported silver catalysts was investigated employing microgravimetric, TPD, and TPR techniques. Analysis of oxygen uptake rates, following the Elovich equation, revealed that three distinct adsorption processes may take place and three distinct oxygen species may coexist on silver surfaces at temperatures and pressures of industrial interest for ethylene epoxidation. One adsorption process, which was dominant at low surface coverages, was found to be essentially nonactivated at zero surface coverage. This process corresponds to dissociative adsorption on multiatom sites. A second adsorption process exhibited an activation energy of 10.5 kcal/mol and corresponds to molecular adsorption on single Ag atoms. A third process was detected at high temperatures, exhibiting an activation energy of 24 kcal/mol and is thought to correspond to subsurface dissolution of oxygen. TPD, TPR, and isotopic labeling studies confirmed the presence of three oxygen species on Ag surfaces and provided evidence for their identification. They also showed that all three oxygen species are active toward ethylene oxidation.

REFERENCES

1. Verykios, X. E., Stein, F. P., Coughlin, R. W., *Catal. Rev.-Sci. Eng.* **22,** 197 (1980).
2. Sachtler, W. M. H., Backx, C., and van Santen, R. A., *Catal. Rev.-Sci. Eng.* **23,** 127 (1981).
3. van Santen, R. A., and Kuipers, H. P. C. E., *in* "Advances in Catalysis" (D. D. Eley, H. Pines, and P. B. Weisz, Eds.), Vol. 35, p. 265. Academic Press, New York, 1987.

4. Grant, R. B., and Lambert, R. M., *Surf. Sci.* **146,** 256 (1984).
5. Campbell, C. T., *Surf. Sci.* **157,** 43 (1985).
6. Campbell, C. T., and Paffet, M. T., *Surf. Sci.* **143,** 517 (1984).
7. Grant, R. B., and Lambert, R. M., *J. Catal.* **92,** 364 (1985).
8. Backx, C., de Groot, C. M. P., and Biloen, P., *Surf. Sci.* **104,** 300 (1981).
9. Campbell, C. T., *Surf. Sci.* **173,** L641 (1986).
10. Rajumon, M. K., Prabhakaran, K., and Rao, C. N. R., *Surf. Sci. Lett.* **233,** L237 (1990).
11. Reijnen, P. H. F., van de Hoek, P. J., Kleyn, A. W., Imke, U., and Snowdon, K. J., *Surf. Sci.* **221,** 427 (1989).
12. Eickmans, J., Goldmann, A., and Otto, A., *Surf. Sci.* **127,** 153 (1983).
13. Pettenkofer, C., Pockrand, I., and Otto, A., *Surf. Sci.* **135,** 52 (1983).
14. Prabhakaran, K., and Rao, C. N. R., *Surf. Sci.* **186,** L575 (1987).
15. Boronin, A. I., Bukhtiyarov, V. I., Vishnevshkii, A. L., Boreskov, G. K., and Savchenko, V. I., *Surf. Sci.* **201,** 195 (1988).
16. Bukhtiyarov, V. I., Boronin, A. I., and Savchenko, V. I., *Surf. Sci. Lett.* **232,** L205 (1990).
17. Chryssikos, G. D., Mattera, V. D., Risen, W. M., and Tsatsas, A. T., *J. Catal.* **93,** 430 (1985).
18. McBreen, P. H., and Moskovits, M., *J. Catal.* **103,** 188 (1987).
19. Anderson, K. L., Plische, J. K., and Vannice, M. A., *J. Catal.* **128,** 148 (1991).
20. Kitson, M., and Lambert, R. M., *Surf. Sci.* **109,** 60 (1981).
21. Toreis, N., Verykios, X. E., *J. Catal.* **108,** 161 (1987).
22. Dean, M., Bowker, M., *J. Catal.* **115,** 138 (1989).
23. Dean, M., McKee, A., and Bowker, M., *Surf. Sci.* **211/212,** 1061 (1989).
24. Dean, M., and Bowker, M., *Appl. Surf. Sci.* **35,** 27–40 (1988–89).
25. Spencer, N. D., and Lambert, R. M., *Chem. Phys. Lett.* **83,** 388 (1981).
26. Backx, C., Moolhuysen, J., Geenen, P., and van Santen, R. A., *J. Catal.* **72,** 364 (1981).
27. Sexton, A., and Madix, R. J., *Chem. Phys. Lett.* **76,** 294 (1980).
28. van de Hoek, P. J., Baerends, E. J., and van Sauten, R. A., *J. Phys. Chem.* **93,** 6469 (1989).
29. Kilty, P. A., Rol, N. C., and Sachtler, W. M. H., *in* "Proceedings, 5th International Congress on Catalysis, Palm Beach, 1972" (J. W. Hightower, Ed.), Vol. 2, p. 929. North-Holland, Amsterdam, 1973.
30. Clarkson, R. B., and Cyrillo, A. C., *J. Catal.* **33,** 392 (1974).
31. Czanderna, A. W., *J. Phys. Chem.* **68,** 2765 (1964).
32. Boghosian, S., Belelis, S., Vayenas, C. G., and Papatheodorou, G. N., *J. Catal.* **117,** 561 (1989).
33. Kondarides, D. I., Papatheodorou, G. N., Vayenas, C. G., and Verykios, X. E., *Ber. Bunsenges. Phys. Chem.*, **97,** 709 (1993).
34. Ioannides, T., and Verykios, X. E., *J. Catal.* **140,** 353 (1993).
35. Taylor, H. A., and Thon, N., *J. Amer. Chem. Soc.* **74,** 4169 (1952).
36. Aharoni, C., and Tompkins, *Adv. Catal.* **21,** 1 (1970).